General Disclaimer

One or more of the Following Statements may affect this Document

- This document has been reproduced from the best copy furnished by the organizational source. It is being released in the interest of making available as much information as possible.

- This document may contain data, which exceeds the sheet parameters. It was furnished in this condition by the organizational source and is the best copy available.

- This document may contain tone-on-tone or color graphs, charts and/or pictures, which have been reproduced in black and white.

- This document is paginated as submitted by the original source.

- Portions of this document are not fully legible due to the historical nature of some of the material. However, it is the best reproduction available from the original submission.

MSC 01500

GRADUATE ENGINEERING PRACTICE

IN MECHANICAL ENGINEERING

Summer Semester 1970

Contract No. NAS 9-10464

Louisiana State University

Mechanical, Aerospace & Industrial Engineering Department

Baton Rouge, Louisiana, 70803

October 15, 1970

cr-114831

LOUISIANA STATE UNIVERSITY
AND AGRICULTURAL AND MECHANICAL COLLEGE
BATON ROUGE · LOUISIANA · 70803

MECHANICAL, AEROSPACE & INDUSTRIAL
ENGINEERING DEPARTMENT

October 15, 1970

National Aeronautics & Space Administration
Manned Spacecraft Center
Houston, Texas 77058

ATTENTION: EW6/A. Louviere

SUBJECT: Contract NAS9-10464, Summer Semester Report

Enclosed is a report on the work performed under contract NAS9-10464 during the summer semester 1970. Any questions may be forwarded to either the program director or associate director.

Charles Teixeira
Charles Teixeira
NASA Associate Director

CT:dbm

Enclosure

APPROVED:

A.R. Mathews for L.R. Daniel Jr.
L. R. Daniel, Jr.
LSU Director

cc: EA/M.A. Faget
EX/M. Silveira
ES/R.E. Vale
EX2/B. Redd
JC42/J.D. Wilcox
BM6/R. Shirkey
BM7/J.T. Wheeler
BM2/C.M. Grant

CONTENTS

FOREWORD

This report presents the results of work performed at Louisiana State University under contract NAS9-10464. This is the second such report under the Graduate Engineering-Practice in Mechanical Engineering program and it covers the analysis performed during the summer, 1970. The participants were Mr. J. Danos, Mr. G. Plaisance, and Mr. J. Rubli. The faculty advisors and lecturers during this period were Professors M. Sabbaghian and A. J. McPhate. The Director of the program was Dr. L. R. Daniel, the Associate Director was Mr. C. Teixeira (NASA-MSC) and the Principal Advisor was Dr. P. H. Miller.

SUMMARY

Three tasks are presently under study by the LSU design team:

1. Separation Techniques--A preliminary design and weight study has been made which shows that a spring loaded ram is an undesirable separation technique due to the very high ratio of weight to separation force. The weight versus energy relationship for a method employing separation rockets on the booster has been obtained and the results indicate that a rocket separation device would weigh considerably less than a spring ram device. A preliminary design of a technique employing a pyrotechnic ram has been included in this report. This method is being studied in more detail.
2. Bulkhead Design--The finite element approach to designing a minimum weight constant stress bulkhead has been refined and completed. Incorporated in the latest formulation are considerations of the principal stresses on the inside and outside of each finite ring, several different failure criteria, and the solution to a sixth degree equation. The derivation of the stress equations on each edge of each finite subdivision of the bulkhead is included in this report. The results of calculations for thickness and deflection are presented for bulkheads fabricated from aluminum and titanium.

3. Propellant Dump--Work has continued on utilizing a thermodynamic model and accompanying computer program which permits a parametric study of the dumping operation. This task will analyze the "unaided" pressure-temperature-time histories in an effort to determine if additional equipment is required in case of an oribter-launch abort.

Flow rate calculations have set the required dump rates at two thousand (2000) pounds per second for the hypothetical one engine configuration and three thousand (3000) pounds per second for the two engine orbiter.

The expulsion retention system proposed in the D. C. 3 report (April 27, 1970) will not be reliable for all abort cases and alternative approaches will be discussed.

I. INTRODUCTION

The following projects are presently being studied:

1. Orbiter/booster separation device
2. Minimum weight "constant stress" bulkhead
3. Orbiter propellant dump

The first task is concerned with selecting a concept and designing the apparatus to separate the two stages of the space shuttle. Design of a minimum weight (simply supported) constant stress circular plate to be used as a propellant tank bulkhead is the second project. The third task deals with dumping the remaining fuel on board the orbiter in the event of a launch abort.

A fourth task--Payload Cannister Design--was terminated in the early part of the summer session because the student involved resigned from the program.

II. DISCUSSION

A. Booster-Orbiter Separation Techniques

1.0 Problem Definition

It is anticipated that four separation schemes will be analyzed:

1. separation by rockets (attached to the booster)
2. spring loaded ram
3. explosive powered ram
4. high speed gas ejector

To date, the first two techniques have been analyzed and their weight/energy relationship has been determined. The results of these analyses are shown in Figure (A-1). The concept for the third technique has been adopted and a set of preliminary design drawings are presented herein. The fourth separation technique is presently being investigated.

2.0 Separation Rockets Attached to the Booster

Any attempt to determine the engine weight and fuel weight for tandem rockets located on the booster wings involves approximations of typical mass fraction and specific impulse data for stage separation rocket engines. The mass fraction, Rmf, is defined as the weight of the rocket propellant divided by the total rocket weight. A reasonable range of values for the mass fraction is from .85 to .90, according to the Propulsion and Power Divison at the Manned Spacecraft Center. The specific impulse, I_s, is

defined as the thrust per unit weight rate of fuel consumption. State of the art upper and lower values of I_s for a rocket exhausting into a vacuum are 300 and 275 $\frac{\text{Lb-sec}}{\text{Lbm}}$, respectively.

2.1 Weight Equation

The total impulse capability of two rocket engines, I_t, is defined as:

$$I_t = 2Ft \tag{A-1}$$

where t = time during which the engine(s) are operating

F = average thrust per engine

It can also be shown that

$$I_t = 2I_s m_f \tag{A-2}$$

where m_f = total mass of fuel for one engine.

From the semester report to MSC dated June 5, 1970, it was shown for a device of this type that

$$F_b t = \sqrt{2m_b E_b} = I_t = 2Ft \tag{A-3}$$

where m_b = mass of the booster

E_b = total energy delivered to the system

F_b = average force on the booster

Setting Equations (A-2) and (A-3) equal results in

$$2I_s m_f = \sqrt{2m_b E_b} \tag{A-4}$$

Therefore, the mass of the fuel for one engine is given by

$$m_f = \frac{\sqrt{2m_b E_b}}{2I_s} \tag{A-5}$$

From the definition of R_{mf}, it can be shown that

$$W_{rocket} = \frac{m_f}{R_{mf}} \tag{A-6}$$

where W_{rocket} = total rocket weight, propellant plus engine structure. Therefore,

$$W_{rocket} = \frac{\sqrt{2m_b E_b}}{2I_s R_{mf}} \tag{A-7}$$

Equation (A-7) shows that the total rocket weight for one engine providing a constant thrust is a function of the mass of the booster, the energy imparted to the booster, the specific impulse of the fuel, and the mass fraction. If one desires to obtain the weight for tandem engines one must multiply by two to obtain

$$W_{2rockets} = \frac{\sqrt{2m_b E_b}}{I_s R_{mf}} \tag{A-8}$$

By using the lower values for the mass fraction and the specific impulse one can plot weight versus energy to obtain a range of heavier and relatively inefficient rockets for the rocket engine design. Employing these parameters for a more efficient engine (high R_{mf} and I_s) will provide the range of the lighter engines. These results are

plotted in Figure (A-1). In these plots the weight of the booster is taken as 450,000 lbm. These results will be compared to the weight/energy results for a spring operated ram device in the following section.

3.0 Spring Loaded Ram

The approach taken in the analysis of the spring loaded ram was the determination of the weight of a helical spring as a function of the desired output final energy.

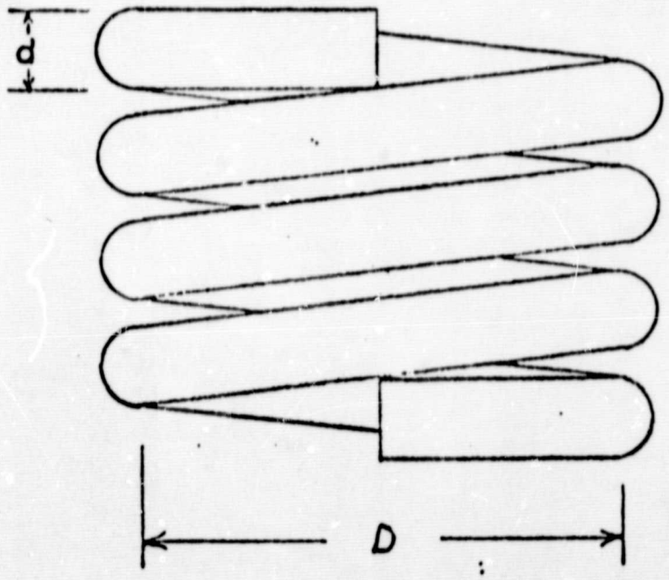

$C = \frac{D}{d}$

SPRING PARAMETERS

Referring to the above sketch the deflection of a helical compression spring is given by

$$\delta = \frac{8Pc^3n}{Gd} \qquad \text{(A-9)}$$

where δ = deflection in inches

P = force in lbs

c = D/d

n = number of active coils

G = modulus of rigidity, lbs/in^2

The energy stored in a spring is

$$E = \frac{P\delta}{2} \tag{A-10}$$

where E = energy in lb-in. Substituting for δ from Equation (A-9) and solving for P results in

$$P = \sqrt{\frac{2EGd}{8c^3n}} \tag{A-11}$$

The maximum stress induced in a spring of this type is given by

$$S_s = \frac{K8Pc}{\pi d^2} \tag{A-12}$$

where S_s = maximum stress lbs/in^2

K = Wahl factor $= \left[\frac{4c-1}{4c-4} + \frac{0.615}{c}\right]$

where $c = \frac{D}{d}$

Replacing P by the expression given in Equation (A-11)

$$S_s = \frac{8K\sqrt{\frac{2EGd}{8cn}}}{\pi d^2} = \frac{4K}{\pi}\sqrt{EG \cdot \frac{1}{cd^3n}} \tag{A-13}$$

Solving for cd^3n,

$$\left[cd^3n\right] = \frac{1f}{\pi^2} K^2 \frac{GE}{S_s^2} \tag{A-14}$$

The weight of a helical spring is

$$W = \rho \frac{\pi d^2}{4} (\pi D) n \tag{A-15}$$

substituting for D = cd,

$$W = \frac{\rho \pi^2}{4} \left[c d^3 n \right] \tag{A-16}$$

Substituting from Equation (A-14) leaves

$$W = \frac{4 \rho G K^2 E}{S_s^2} \tag{A-17}$$

Since we are attempting to find the lightest spring, we need K and $\frac{\rho G}{S_s^2}$ to be minimum. As c becomes large, K approaches 1 asympototically (Reference 1). Therefore, K = 1 was used as an upper limit since no spring could be designed which would be lighter than one corresponding to this condition.

In order to minimize $\left(\frac{\rho G}{S_s^2}\right)$, we first note that for most spring steels, ρ = .285 lbm/in^3. Also, G = 10.5 x 10^6 lbs/in^2 for hot wound springs and G = 11.5 x 10^6 lbs/in^2 for most cold drawn springs. To maximize S_s^2 we refer to Figure 23 of Reference 1. The largest value for the allowable stress occurs at d = .5 in. and is equal to 130,000 lbs/in^2. The spring material is hot wound SAE 6150 or SAE 9260.

a brief review of these problems and possible solutions to them. The reasons for choosing a particular solution will also be explained.

The basic concept of the explosive powered ram separator is as shown in Figures (A-2) and (A-3).

4.1.1 Force and Time

Discussions with NASA personnel working in the Structures and Mechanics Division revealed that an increasing separation force proportional to some power of time may be desirable from a vibrational standpoint. In order to determine if any state of the art designs for regulating force were available, conversations with personnel in the Propulsion and Power Division revealed that there were several methods for accomplishing this. The following techniques were suggested:

1. crushable honeycomb
2. variation in the velocity by using a type of "shock absorber" mechanism similar to that utilized on the escape hatch for Apollo
3. variation in propellant type
4. variation in propellant configuration
5. eroding of the inlet nozzle by the flowing gas

Since the first two techniques involve relatively high energy losses, they were considered undesirable. The next two ideas are within the peripheral state of the art and experimentation could conceivably produce the desired output. The last technique has also been successfully demonstrated under experimental conditions.

Since the last three methods are not fully developed, no one technique will be selected at this time. Instead, a preliminary design will be developed which will be adaptable to any combination of the three techniques.

One possible approach to the eroding nozzle technique would be to employ nozzles of varying diameter around the cylinder walls. As the piston is displaced more and larger nozzles would be opened to admit the gas which provides the force on the piston.

The hardware connecting the combustion chamber and the ram will be provided in this initial layout but no facilities will be developed to provide for any variance in type or configuration of the propellant.

4.2.0 Separation Procedure

To initiate the separation, the frangible nut, shown in Figure (A-2), is broken by the use of an explosive device. Immediately afterwards, the charge used to separate the vehicles is ignited and member two is forced upwards by the gas pressure being released through the ports at the lower end of member three, a pressure vessel. Since choked flow conditions would be present in all gas ports exposed as member two proceeds upwards, more and larger gas ports become available for the pressurization of the increasing space between members two and three. This, together with a pyrotechnic device capable of varying the pressure versus time to the first or second power, should give a force output proportional to even larger powers of time, for small time increments.

Next, as shown in Figure (A-3), the stop spring between members one and two prevents member two from leaving member three. Finally, as the orbiter moves away from the sealed ram head of member two, gas pressure is released from the top of member two. The small slot near the bottom of member one allows the gas to exit as member two returns to its initial configuration.

4.2.1 Gas Port Sizes and Orientation

After the dimensions of the constituent parts of the lightest weight ram device (see Sec. 4.4) are determined, it is anticipated that a computer program will be devised in order to optimize the size and orientation of the inlet ports located in the walls of member three.

4.2.2 Advantages of the Explosive Powered Ram Concept

The following aspects of the design shown in Figure (A-2) and (A-3) are regarded as inherent advantages:

1. Redundancy--more than one explosive device may be used for the frangible nut.
2. Paucity of moving parts--only one member is required to undergo a displacement.
3. Double purpose--this ram concept also acts as a device capable of attaching orbiter and booster together when combined with hardware located aft of both vehicles.
4. Lightweight--the following aspects of this design contribute to its light weight.
   (a) large amounts of inertia at Section B--provide for maximum moments, (see Section 4.3.2)

(b) large area used to support load at Section B--whole ram need not support orbiter on the ground (see 4.3.1)

(c) the large moment of inertia--area for member two.

5. Force time output--three aspects need to be considered:

(a) the increasing area as member two proceeds upwards prevents a large initial force

(b) size and orientation of nozzles can produce nearly any desired force-time history

6. Automatic ram retraction--the release of pressure through the ram head need not be controlled by the booster crew.

4.3.0 Strength Calculations

Since the various components of the ram separator will undergo stresses of varying magnitudes and directions throughout the mission, three distinct force-reaction cases must be analyzed.

4.3.1 Ground Loads

The forces acting on the ram while the shuttle is in a horizontal altitude are shown in the following sketch. The shoulder designated "A" in Figure (A-3) is designed to withstand all of this compressive load, so that this force is not transmitted to members below it.

Force-Reaction Diagram

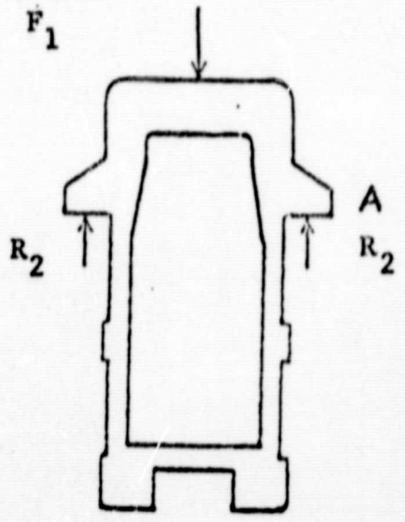

F_1 is caused by the weight of the orbiter

Case 1--On the ground in horizontal position.

4.3.2 Launch Loads

At some time during the assent phase of flight the force F_3 shown in the following sketch is a maximum, being composed of an inertia term, that portion of the weight of the orbiter supported by the ram, and the maximum drag on the orbiter. The moment about point "0", M', is provided to account for the disparity in the moments of booster and orbiter. The direction of this moment is assumed, pending calculations. A side load, F_4, is also included to account for sudden lateral wind conditions. It is believed that the maximum bending moment on member 2 will occur at a section in the immediate vicinity of shoulder "A".

Force-Reaction Diagram

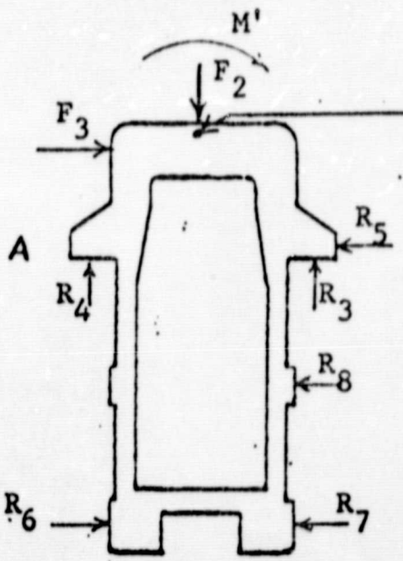

...used by drag and

...er weight

Case 2--During take off

4.3.3 Separation Loads

The major forces acting on the ram at normal separation are shown in the following sketch. The dynamic pressure is only ≈ 1 lbf/ft^2 at this altitude; hence, loads are negligible, and only a normal explosion force, F_e, and the reaction, R_e, are considered significant.

Force-Reaction Diagram

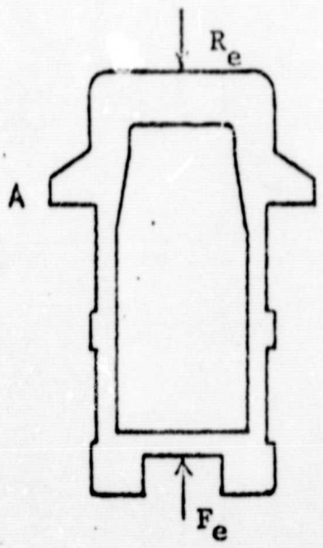

Case 3--At Separation

F_e = max. thrust caused by the pyrotechnic device pressure

Since several of the force-reaction diagrams shown above involve indeterminate situations, a method which first assumes one force is zero and then solves for the other one will be utilized. A moment diagram will then be drawn for this case. Next another force will be assumed zero and the others determined. A moment diagram will again be drawn. Finally, a composite diagram will be constructed for each of the critical loading conditions.

4.4 Least Weight Ram

Personnel at the MSC concur that if a separation device of the type being considered (Explosive Ram) were to be used, the structures could withstand a separation force of 100,000 lbs. The stroke being suggested by MSC varies from 1.5 to 3.0 feet with 2.0 feet being used most often in recontact simulation studies. Thus, the energy delivered by such a system can be from 150,000 to 300,000 ft-lbf. However, during the first phase of this design, the design energy output will be 200,000 ft-lbf.

The variable to be minimized is the ram weight, including the combustion chamber but not including the support structure required in the booster and orbiter. The controlling factor for the minimum weight is the maximum ram force and hence final ram pressure. If a small pressure were to be used to obtain a final force of 100,000 lbf., the diameter of member two would be large. This means a large diameter for members 3 and 4 even though the walls of these vessels need not be thick. Utilizing a larger pressure would mean thicker walls for members two, three, and four but their diameters would be smaller. One may recall that for a specific outside diameter cylinder, weight increases approximately linearly with wall thickness (small thickness).

The above stated problem is ideally suited for a computer iteration procedure and a program is now being written to solve it.

5.0 Conclusions

Figure (A-1) graphically shows that the spring activated ram is an undesirable technique from a weight standpoint. The range of weights

for tandem rocket engines is also shown. A preliminary concept for the pyrotechnic powered ram has been adopted and is shown in Figures (A-2) and (A-3). The force diagrams which will be utilized to determine the necessary dimensions on the ram components are presented in section (4-3). The optimization scheme which will initially be used to design a minimum weight ram has been explained in Section 4.4.

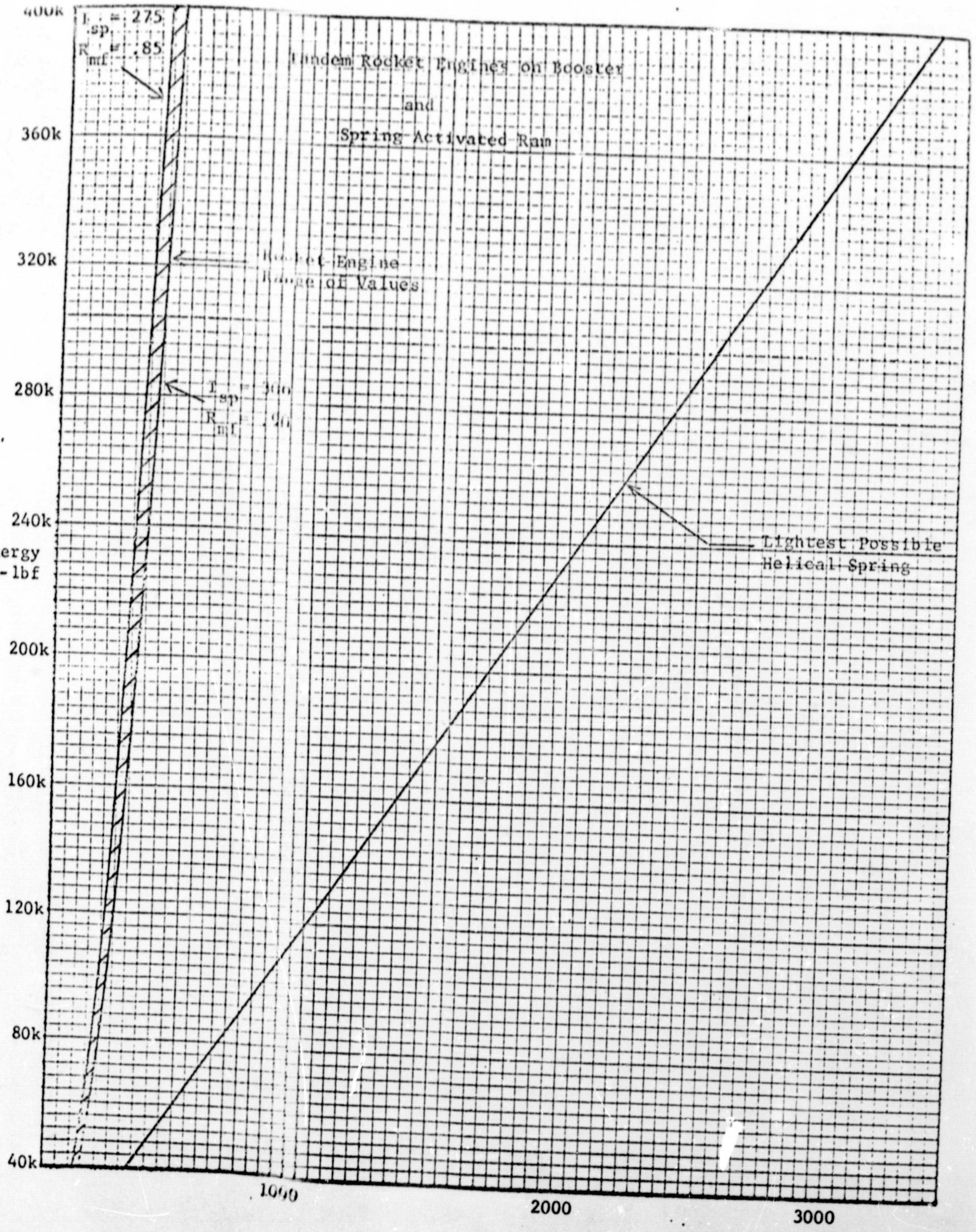

Figure (A-1)

SEPARATION ENERGY VERSUS SYSTEM WEIGHT

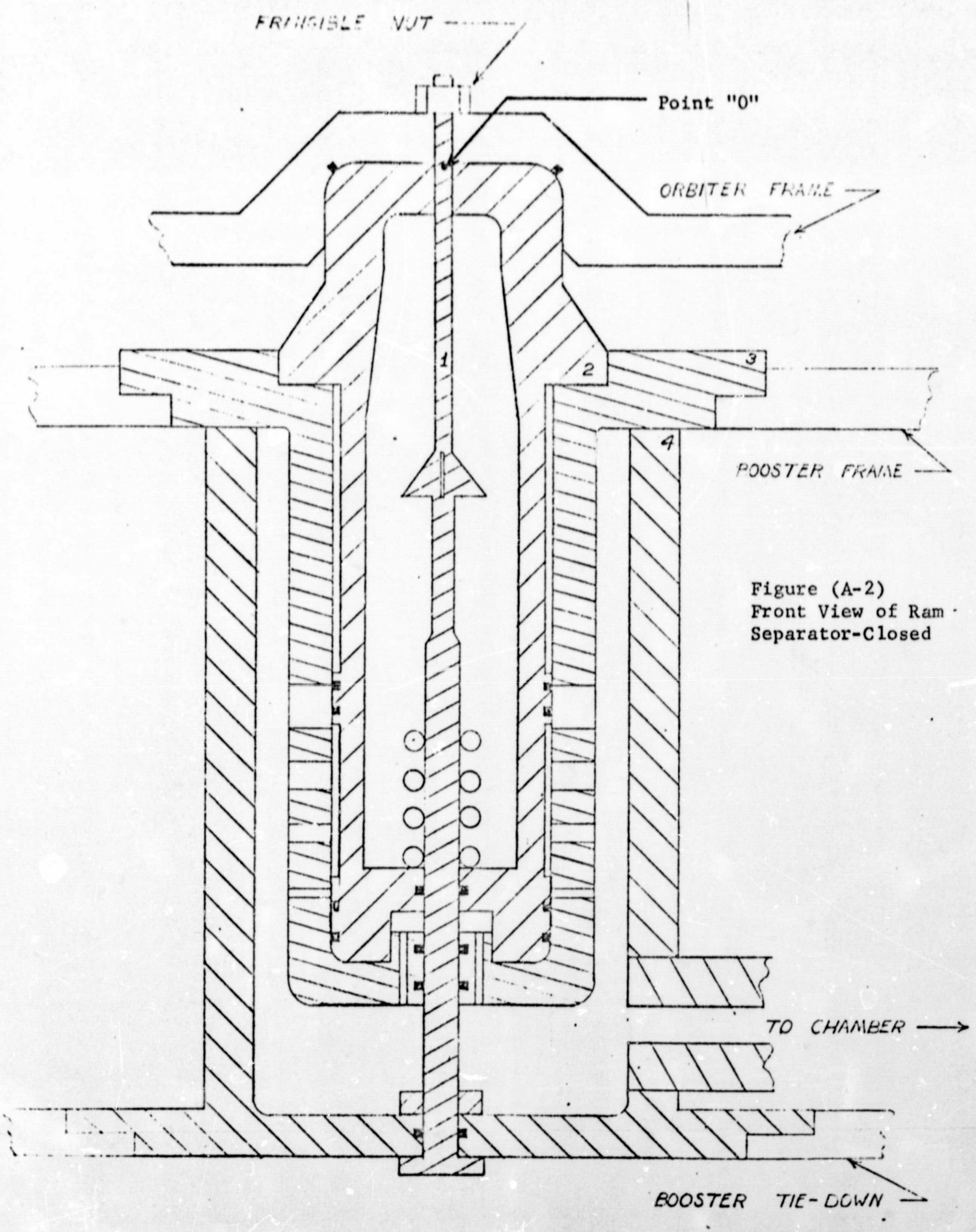

Figure (A-2)
Front View of Ram
Separator-Closed

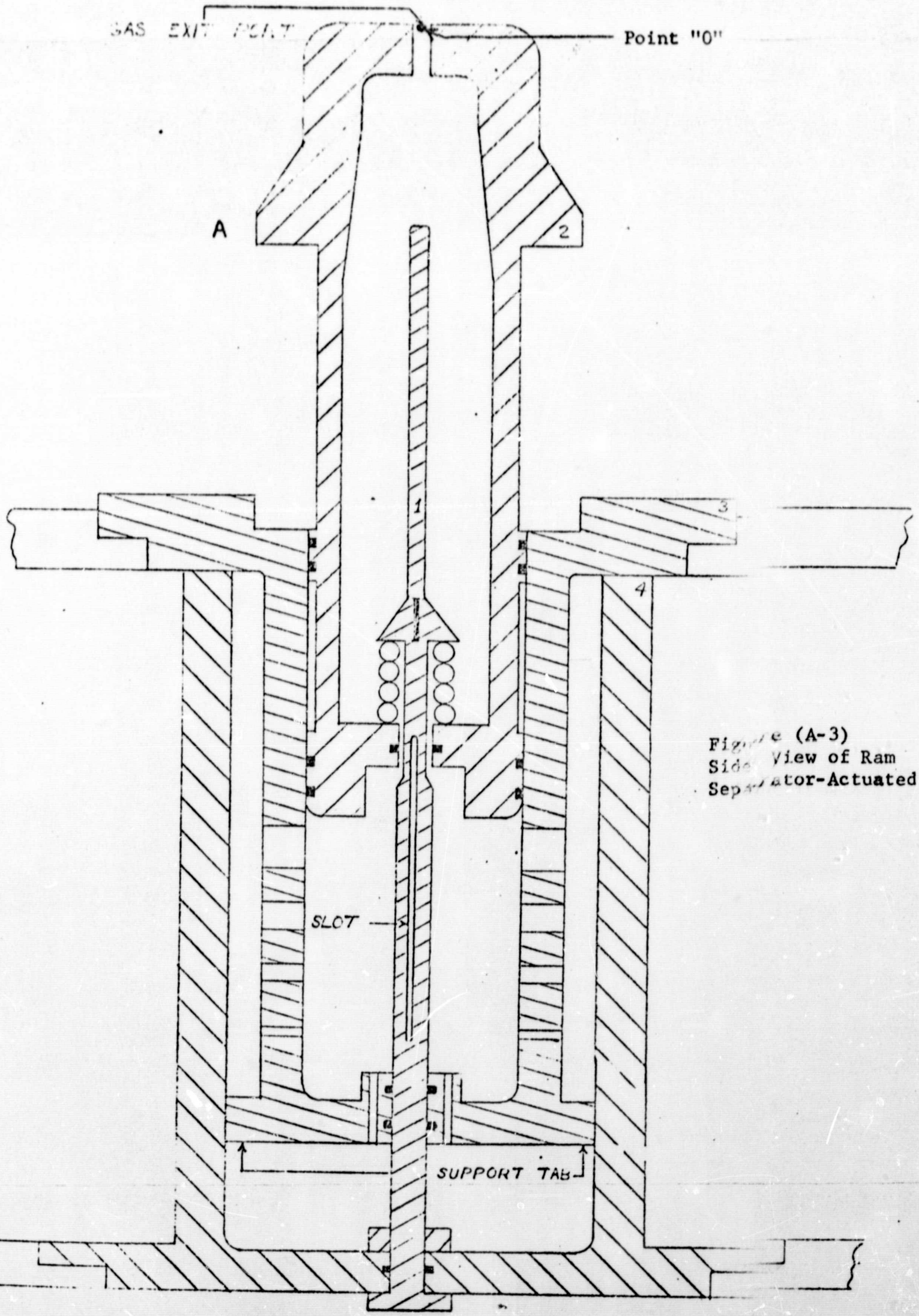

Figure (A-3)
Side View of Ram
Separator-Actuated

B. Constant-Stress Circular Plate for Space Shuttle Applications

Problem Definition

The work done during the past summer on the constant-stress circular plate involved refining the computer approach to the finite ring method discussed in the spring semester report. This method involves dividing the plate into many rings each of which has a constant thickness. The thickness of each ring is calculated based on principle stresses both on the inside and outside edge of each ring. It is possible to calculate the thickness using the following failure theories: maximum strain energy, shear-distortion (Hencky-Von Mises), and the maximum-normal stess theory.

An earlier version of the computer program involved solving a cubic equation for the thickness of each ring by the maximum-normal-stress failure theory. In the present program, in order to include the other two aforementioned theories, it is required to solve a sixth degree equation. Calculation of both the deflection of each ring and the total deflection is another feature included in the present program.

The derivation of additional stress equations for the inside and outside edge of each ring as presently used in the computer program will be discussed in detail.

Derivation of Programmed Equations

The loads on each ring were divided up into three parts, pressure loads, shear loads, and uniform edge moments. The two

principal stresses at the inside edge and outside edge of each ring were required in the calculation. Each of these stresses contained components from the three types of loads. The equations for the stresses on the outside edge were derived with the aid of Reference 2 & 3. The following is an outline of those derivations:

Simply supported ring with shear loads:

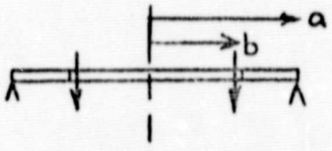

The tangential stress is given by the following equation:

$$\sigma_t = \frac{6m_t}{t^2}$$

where m_t is the moment acting on the plate and it can be represented by:

$$m_t = -D\left(\frac{1}{r}\frac{dw}{dr} + v\frac{d^2w}{dr^2}\right)$$

The slope $\left(\frac{dw}{dr}\right)$ is given by the following equation where C_1 and C_2 are constants of integration

$$\frac{dw}{dr} = \frac{Pr}{8\pi D}\left(2\log\frac{r}{a} - 1\right) - \frac{C_1 r}{2} - \frac{C_2}{r^2}$$

$$\frac{d^2w}{dr^2} = \frac{P}{8\pi D}\left(2\log\frac{r}{a} - 1\right) + \frac{P}{4\pi D} - \frac{C_1}{2} + \frac{C_2}{r^2}$$

From boundary conditions C_1 and C_2 can be represented as:

$$C_1 = \frac{P}{4\pi D}\left(\frac{1 - v}{1 + v} - \frac{2b^2}{a^2 - b^2}\log\frac{b}{a}\right)$$

$$C_2 = -\frac{(1 + v)P}{(1 - v)4\pi D}\frac{a^2b^2}{a^2 - b^2}\log\frac{b}{a}$$

Substituting for m_t in the stress equation gives the following result:

$$\sigma_t = -\frac{6D}{t^2}\left[\frac{1}{r}\frac{dw}{dr} + v\frac{d^2w}{dr^2}\right]$$

Substituting for $\frac{dw}{dr} + \frac{d^2w}{dr^2}$ and simplifying results in the following equation:

$$\sigma_t = -\frac{6D}{t^2}\left[\frac{P}{4\pi D}\log\frac{r}{a}(1+v) + \frac{P}{8\pi D}(v-1) + \right.$$

$$\left. -\frac{C_1}{2}(1+v) - \frac{C_2}{r^2}(1-v)\right]$$

which after substituting for C_1 and C_2 becomes:

$$\sigma_t = \frac{3pb^2}{2t^2}\left[\log\frac{a}{r}(1+v) + (1-v) + \frac{b^2(1+v)}{(a^2-b^2)}\log\frac{a}{b}\left(1+\frac{a^2}{r^2}\right)\right]$$

$$\sigma_{t_{r=a}} \frac{3pb^2}{2mt^2}\left[(m-1) + \frac{2b^2(m+1)}{a^2-b^2}\log\frac{a}{b}\right]$$

where

σ_t = stress in tangential direction

m_t = bending moment per unit length acting on the diamental sections of the plate

t = thickness of plate

w = deflection of plate

r = radius at any given point on plate

a = outside radius of plate

b = inside radius of plate

D = flexural rigidity of the plate

C_1&C_2 = constants of integration

v = Poisson's ratio

m = 1/v

P = load on plate in lbs

p = pressure on plate in psi

The stress on the following simply supported ring with a pressure load is desired.

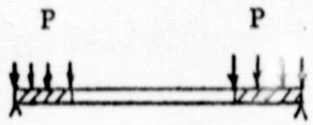

This case was done by superimposing the following three loads:

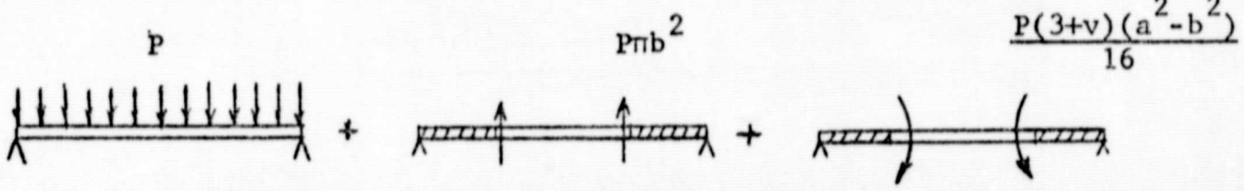

where the stress equations for the three loads are given respectively by:

Pressure:

$$\sigma_{t_{r=a}} = \frac{3pa^2}{8mt^2}\left[(3m + 1) - (m + 3)\right]$$

Shear:

$$\sigma_{t_{r=a}} = \frac{3pb^2}{2mt^2}\left[(m - 1) + \frac{2b^2}{a^2 - b^2}(m + 1)\log\frac{a}{b}\right]$$

Moments:

$$\sigma_{t_{r=a}} = \frac{6}{4mt^2(a^2 - b^2)}\left[\frac{p(3 + \nu)(a^2 - b^2)}{16} b^2 (2)\right]$$

adding these and simplifying results in:

$$\sigma_{t_{r=a}} = \frac{3p}{4mt^2(a^2 - b^2)}\left[a^4(m - 1) - b^4(m + 3) + \right.$$

$$\left. + 4a^2b^2 - 4b^4(m + 1)\log\frac{a}{b}\right]$$

The plate is made up of a center disk and many constant thickness rings. The procedure involves making an initial estimate of the thickness of the center disk and performing the calculations for the

thickness of each ring, the slope of the edges of each ring and the moments on the edges of each ring. The constraint that had to be met was that the moment on the outside edge of the outermost ring be zero (simply supported). If this iteration of the outside edge moment of the outermost ring is not zero then the initial estimate of the center disk thickness was wrong and another estimate must be made for the center disk thickness. To minimize this iteration process, the initial estimate was chosen as 1.5 times the thickness calculated based on constant thickness equations for the entire plate. Using this value as an initial estimate for the center disk, the procedure was to decrease this thickness until the moment on the outside edge of the plate was zero.

Results:

From the number of runs obtained it appears that the design based on maximum stress or distortion energy will result in a relatively large deflection for a material with very high yield stress and a low modulus of elasticity. For these materials, the optimum profile is not thick enough to provide the stiffness required for small deflections. The pressure load also has a large effect on deflections. For higher pressures the required thickness becomes larger thus making the plate more rigid and there is less deflection.

An extreme example of some of the large deflections obtained was the case of a 200 inch diameter titantium plate ($\bar{\sigma}$ = 155,000 psi) under 20 psi of pressure which gave a deflection of 54 inches. The

equations used in the program are based on small deflection theory and since this is not a small deflection the results are not truly accurate. However, the results are such that they do show the order of magnitude of the deflection. It is noted that for higher pressures the deflection becomes less, because the thickness is greater therefore increasing the modulus of rigidity. From the practical standpoint it may be necessary to add a new constraint to the problem, that of maximum acceptable deflection.

The deflection and thickness profile for an aluminum bulkhead are given in Figures B1 and B2. These results show that for a yield stress of 45,000 psi the deflections are within small deflection theory.

A preliminary conclusion which can be drawn is that if the yield stress is fairly low then the results produced are accurate since they are in the small deflection range.

FIGURE B-1 - NORMALIZED DEFLECTION VERSUS NORMALIZED RADIUS

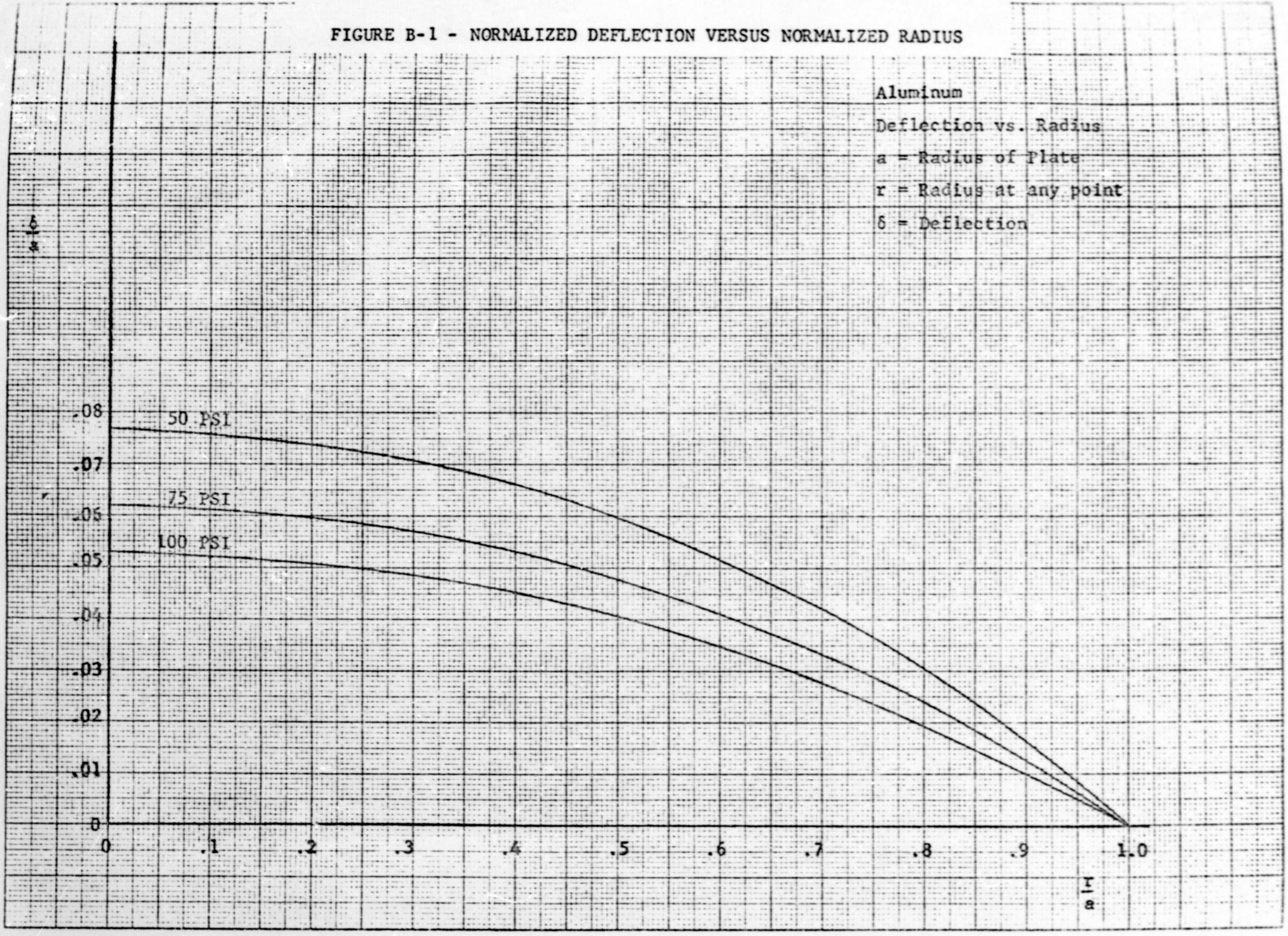

FIGURE B-2 - NORMALIZED THICKNESS VERSUS NORMALIZED RADIUS

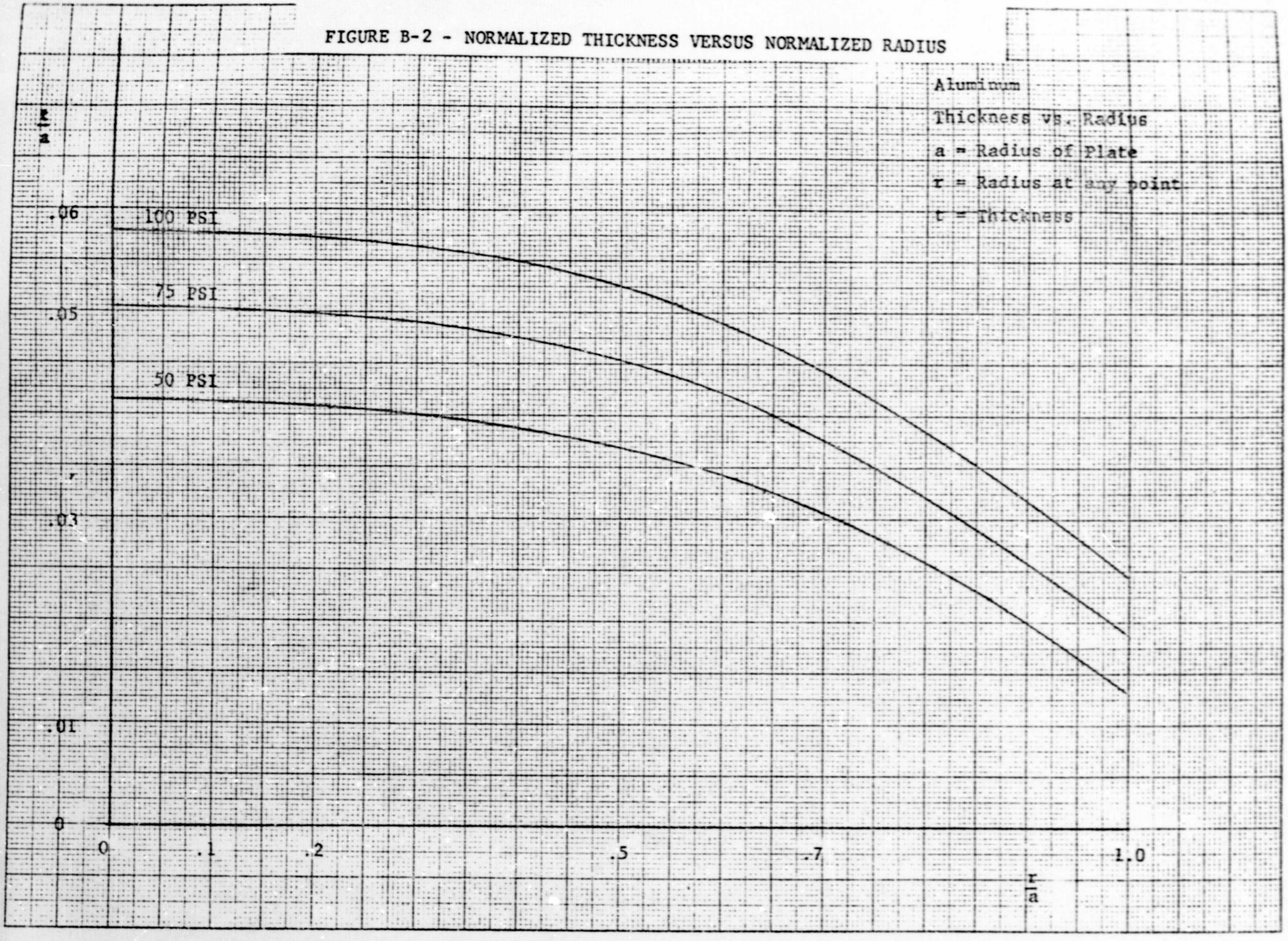

C. Orbiter Propellant Dump

Problem Definition:

For the safety of the orbiter crew, it is necessary to study all possibilities of failure in any or all elements of each critical system. In the event of loss of thrust (and therefore propellant tank pressurization) a catastrophic condition may exist upon attempted reentry of a fully or partially fueled vehicle into the earth's atmosphere. It is therefore necessary to provide a capability to dump the remaining propellant before the severe reentry problems are encountered.

Three areas of interest were studied during the summer semester. Since it will be necessary to predict the formation of solid material (dense slush or frozen materials) in the propellant and oxydizer tank, major work encompassed the development of a thermodynamic tank model to be used on the IBM 360-65 series computer at Louisiana State University. Secondly, study was completed to decide upon a flow rate design parameter for the liquid expulsion system. The final portion of the summer's activity involved examination of the physical hardware and design of a positive expulsion device to assure liquid flow from each cryogen tank.

1.0 Tank Model and Thermodynamic Analysis

As noted in the first report under this contract, Reference [4], the Residual Propellant Orbital Thermodynamics Program (REPORTER) was thought to include all necessary characteristics to predict the thermodynamic-time history within the propellant and oxydizer tanks. A card record of a source program and documentation have been obtained through

the Complab section of Marshall Spaceflight Center. The documentation, Reference [5], is convincing that REPORTER can give the required results. The results obtained using the model have correlated quite well with vapor venting data in Saturn IV stage flights and liquid venting data from Centaur vehicle flights with twenty-two (22) percent fuel residuals.

Modifications of some Fortran statements were necessary due to system inconsistancies of the IBM 7094 at Huntsville and IBM 360 at LSU. The modifications have been completed. Data pertinent to the orbiter dumping problem are now being collected. Data inputs include:

1. tank geometry,
2. heat input of each phase of cryogens,
3. thermodynamic properties of the cryogens,
4. material quality mass ratio of vapor to total mass at nozzle exits,
5. characteristics of vapor venting valve(s)

Data items one through four have been researched sufficiently to allow initiation of the model. The last item, the characteristics of the vapor vent(s), has not been finalized. It is thought several types might be modeled. Further discussions follow where deemed necessary.

1.1 Tank Geometry

The tank geometrical model will use an average nominal radius of fifty inches (50") on two parallel tanks instead of the sixty by forty inch (60"/40") "double-bubble" tank configuration. The twin

parallel hydrogen tanks are capped with hemispherical ends. The twin parallel oxygen tanks are capped with an inverted hemispherical head on the drain end and a hemisphere on the forward end. Figure C-1 illustrates this concept and notes the ten equal volume nodes to be used.

A flow circuit from the tank to the vent nozzle on the vehicle skin could be modeled as a part of the main tanks. This procedure is questionable at present because of uncertainty as to quality of the two (or possibly three) phases in the pipe. Further examination of these problem areas are needed prior to a final decision.

1.2 Heat Input

Heat input to tank walls and contents will be based on data obtained from the S-IVB stage heating using a forty percent reduction in flux due to the shuttle outer skin as recommended in Reference [6].

1.3 Nozzle Size

Sizing of the nozzles for liquid expulsion will result from data retrieval of the REPORTER. For initial attempts, it is thought that an eight (8) inch line should be examined. This choice was made due to the eight (8) inch line size specification on both the propellant and oxydizer feed systems as noted in Reference [6]. In this way, it is hoped that the tank feed ports may also act as vent ports, in the case of abort. Although the eight (8) inch vent is not known to be the exact requirement, it will provide the needed initial reference point for future decisions. This scheme would require no additional wall perforations in either tank.

1.4 Phase Quality

The phase quality at nozzle exits requires an assumption. It is considered that the high flow rates required to aid in successfully aborting the mission can only be achieved if total liquid or nearly total liquid is expelled. For this reason it is assumed that if two phases, gas and liquid, flow occurs at the nozzle the ratio of liquid to gas is greater than nine to one or a quality of 0.1 or ten percent (10%) exists. In order to assure that this condition is satisfied, it will be necessary to recommend the addition of hardware to the tankage structure. A discussion of this problem follows in section 3.0.

2.0 Flow Rate Determination

The flow rate for abort system design was calculated for one and two engine orbiter configurations by orbital maneuver methods. In Reference [4], a flat earth approach to this problem was formulated and results presented. These results, with the time after separation in seconds as the abscissa, are shown again in Figure C-2 for completeness. Figures C-3 and C-4 present the elliptical trajectory approach results from the hypothetical one engine and the normal two engine concepts. No set of flat-earth ballistic calculations were made for the two engine concept due to the similarity of results with those of the more realistic orbital approach as noted in the one engine case.

Results dictate that the flow rate required in the hypothetical (i.e. one engine) orbiter abort is approximately two thousand (2000) pounds per second for 100 seconds. Likewise a two engine orbiter abort would require a system designed to accommodate approximately three thousand (3000) pounds per second for 100 seconds.

3.0 Positive Expulsion System

It is suggested in Reference [6] that orbiter engine ignition be accomplished without an ullage maneuver to settle the propellants. It is proposed that this be done using two passive retention screens. One screen is to be located just below the one-G liquid vapor interface. A second screen, to be located near the tank outlets, will serve as a redundant measure and for flow control. As these elements have not been sufficiently described, it is the purpose of this section to discuss what is thought necessary in more detail.

The requirements of the retention and expulsion system are twofold.

1. Prevent excessive propellant and oxydizer sloshing that may affect vehicle dynamic stability.
2. Provide for total or nearly total liquid expulsion from each tank.

The two screen suggestion would accomplish this criteria in the case of a typical ignition but could fail in abort conditions for several reasons. To understand how failures in the abort regime could occur it is best to explain the typical mode of operation and note differences in abort modes that may cause problems.

Propellant slosh will occur at booster-orbiter separation due to tank wall rebound and liquid inertia. At that time there is only slight acceleration due to applied or body forces. The approximate order of magnitude of accelerations are listed below (Reference [7]).

Source	
1. Aerodynamic Drag	$10^{-6} - 10^{-7}$ ft/s^2.
2. Radiation Pressure from sun	$10^{-8} - 10^{-9}$ ft/s^2.
3. Gravity of earth	$10^{-4} - 10^{-5}$ ft/s^2.
4. Centripetal acceleration	$10^{-5} - 10^{-6}$ ft/s^2.

Toole and Hastings, Reference [8], have hypothesized that the maximum amplitude of a sloshing propellant is given by Equation 1.

$$\delta \approx 0.74 \, V_f \left[\frac{R}{a}\right]^{\frac{1}{2}} \tag{1}$$

where δ = maximum sloshing amplitude

V_f = fluid velocity (with respect to the tank)

R = characteristic radius

a = magnitude of acceleration regime.

For a tank, without retention aids, R is defined as the tank radius, in this case fifty inches (50"). To include a screen retainer at the liquid vapor interface allows the characteristic radius to be the wetted radius of the screen, which is on the order of microns. As noted from Equation (1), as R is decreased so is δ decreased.

If, however, the low acceleration level is suddenly applied after liquid-vapor interface falls below the screen, the characteristic radius again refers to the tank radius. In essence, the screen is the "top" of the tank. This situation is exactly the one which may occur if boost engines fail after ignition and burn time. Thus in the abort regime, if

entered after some engine burn, the "top" screen becomes obsolete as an anti-sloshing device. The problem is compounded due to possible vapor bubble entrapment as the liquid sloshes and splashes about in the tank.

Due to the wall wetting quality of both liquid oxygen and hydrogen the possiblity exists that the most stable configuration for the system is one with most fluid about the stabilizing "top" screen as seen in Figure C-5. With most liquid away from the vent port, the low quality expulsion is impossible.

These conditions imply the proposed retention and expulsion system, while adequate for nominal insertion boost engine start, will not be sufficiently reliable in considering all abort condition possibilities.

A revised retension system is to be studied that is believed to positively vent the liquid cryogens at necessary flow rates.

The requirement of the system is one of low quality (below 10%) liquid expulsion at flow rates needed for abort conditions (2000 to 3000 lb/sec) with no hinderence to normal system operation. The most effective system would be a perforated inner wall of either fine mesh screen or stamped metal sheet. This system would form an annular space which could be designed to allow only liquid expulsion for any acceleration environment. Discussions on this type of containment and orientation system can be found in Reference [9], [10], and [11]. However, because of weight penalties that would result in a complete liner, this system is deemed unsatisfactory.

As a weight to efficiency tradeoff, it is thought that either one of the two following systems will effectively satisfy flow conditions in the abort situations; however, the better of the two systems cannot be specified at this time. One configuration involves an interconnected arrangement of screened panels. This system partitions the tank wall into sections that will locate liquid at screens and supply sizable flow rates to the vent nozzle(s) from any location.

The second system uses a spiraled screen "pipe" near the tank wall contour and also along the tank centerline, if necessary.

Neither of these systems will solve the problem of dynamic stability in the abort mode. Further studies are needed prior to the making of a final recommendation.

HYDROGEN TANK MODEL

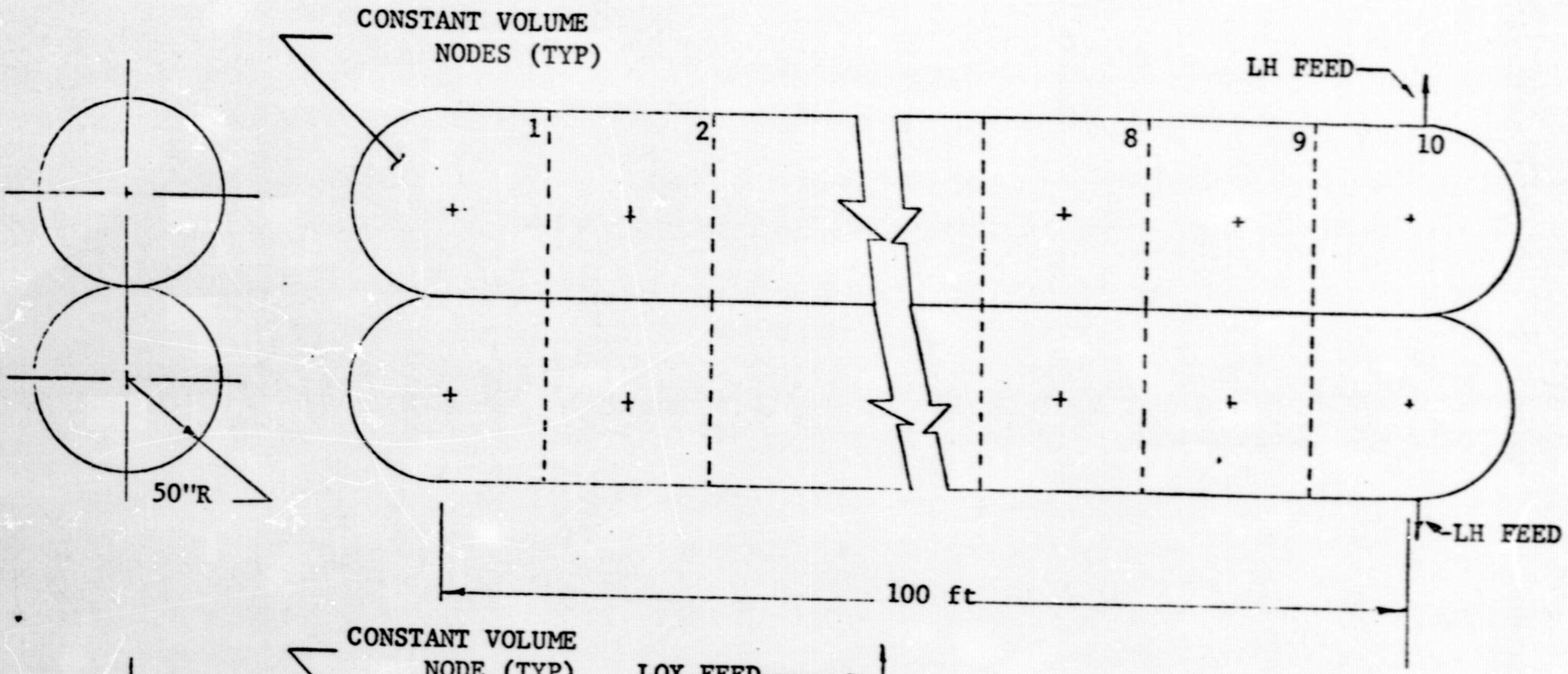

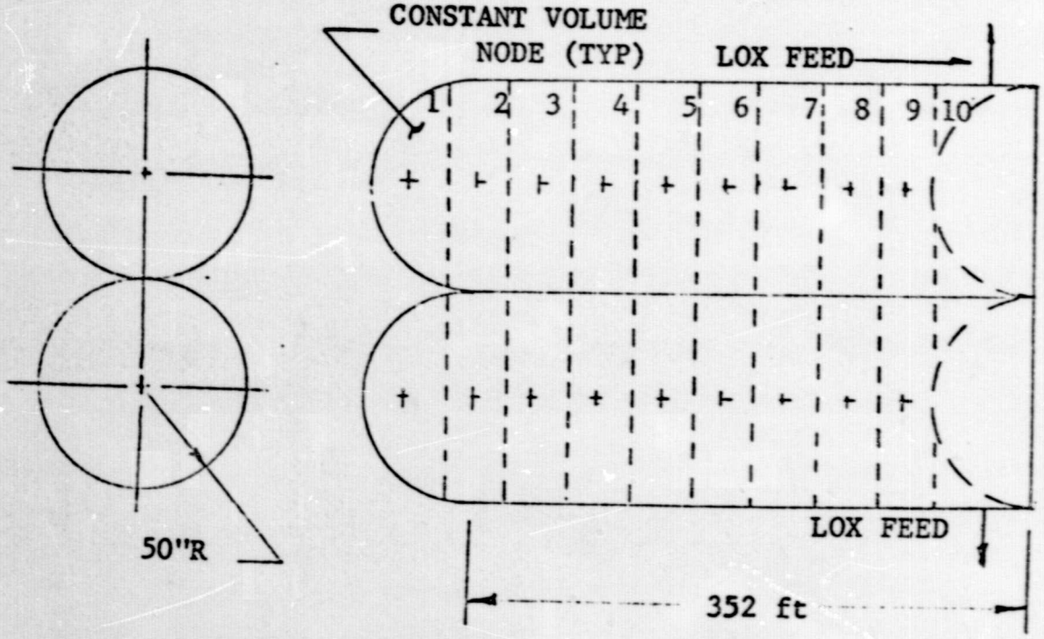

OXYGEN TANK MODEL

FIGURE C-1

MODELING CONFIGURATION
OF LOX AND LH
TANKAGE

TIME OF ABORT AFTER SEPARATION	DUMP TIME	DUMP RATE
0.0	81.11	1954.05
25.0	83.00	1714.39
75.0	77.51	1419.39
125.0	67.03	1159.71
175.0	56.25	808.16
	52.23	252.24

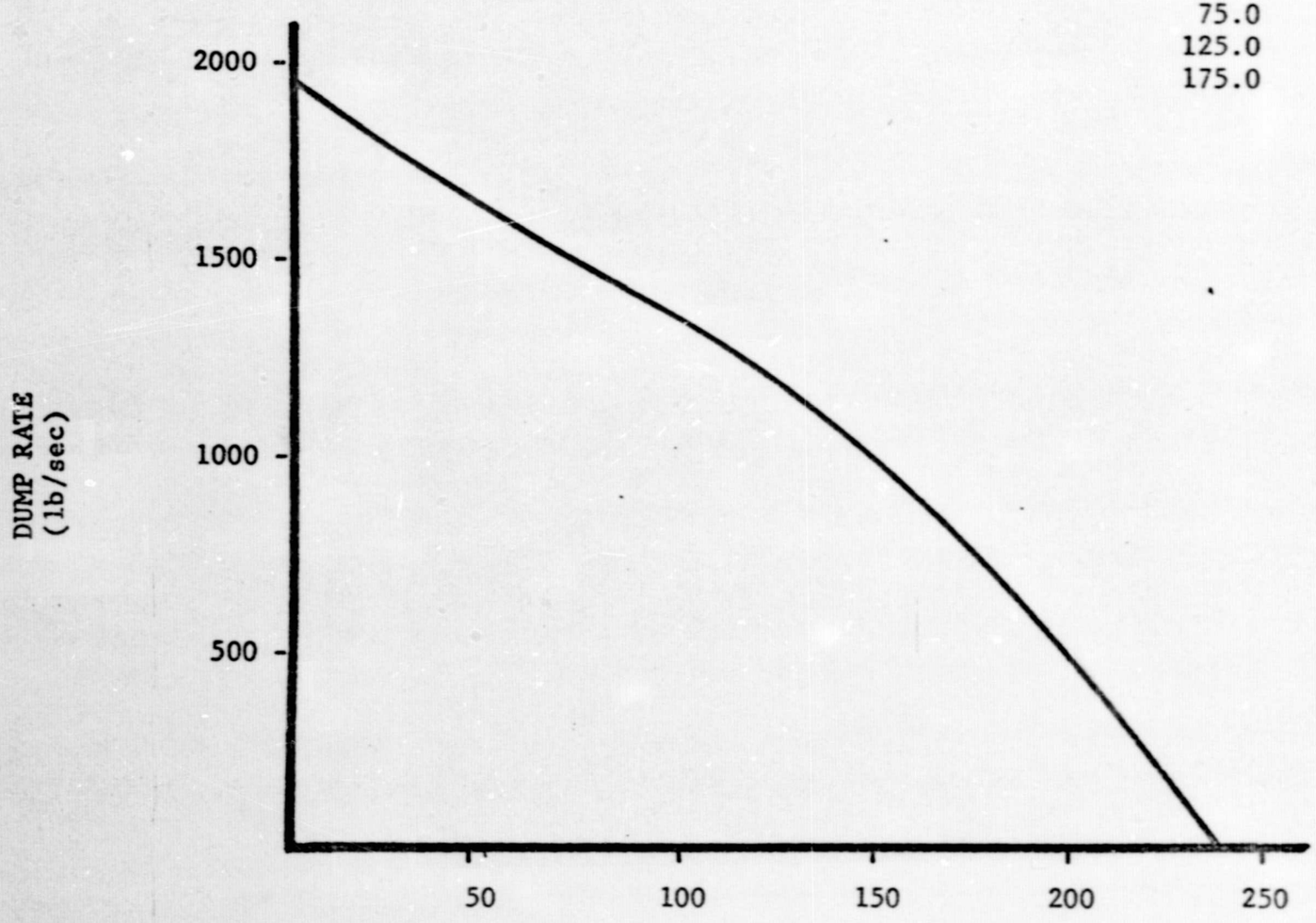

FIGURE C-2

FLAT-EARTH DUMP RATES FOR ONE ENGINE ORBITER CONFIGURATION

TIME OF ABORT AFTER SEPARATION	DUMP TIME	DUMP RATE
0.0	92.4	1622.44
25.0	94.2	1419.12
75.0	89.9	1127.97
125.0	81.1	853.63
175.0	75.8	487.22
275.0	106.2	44.03

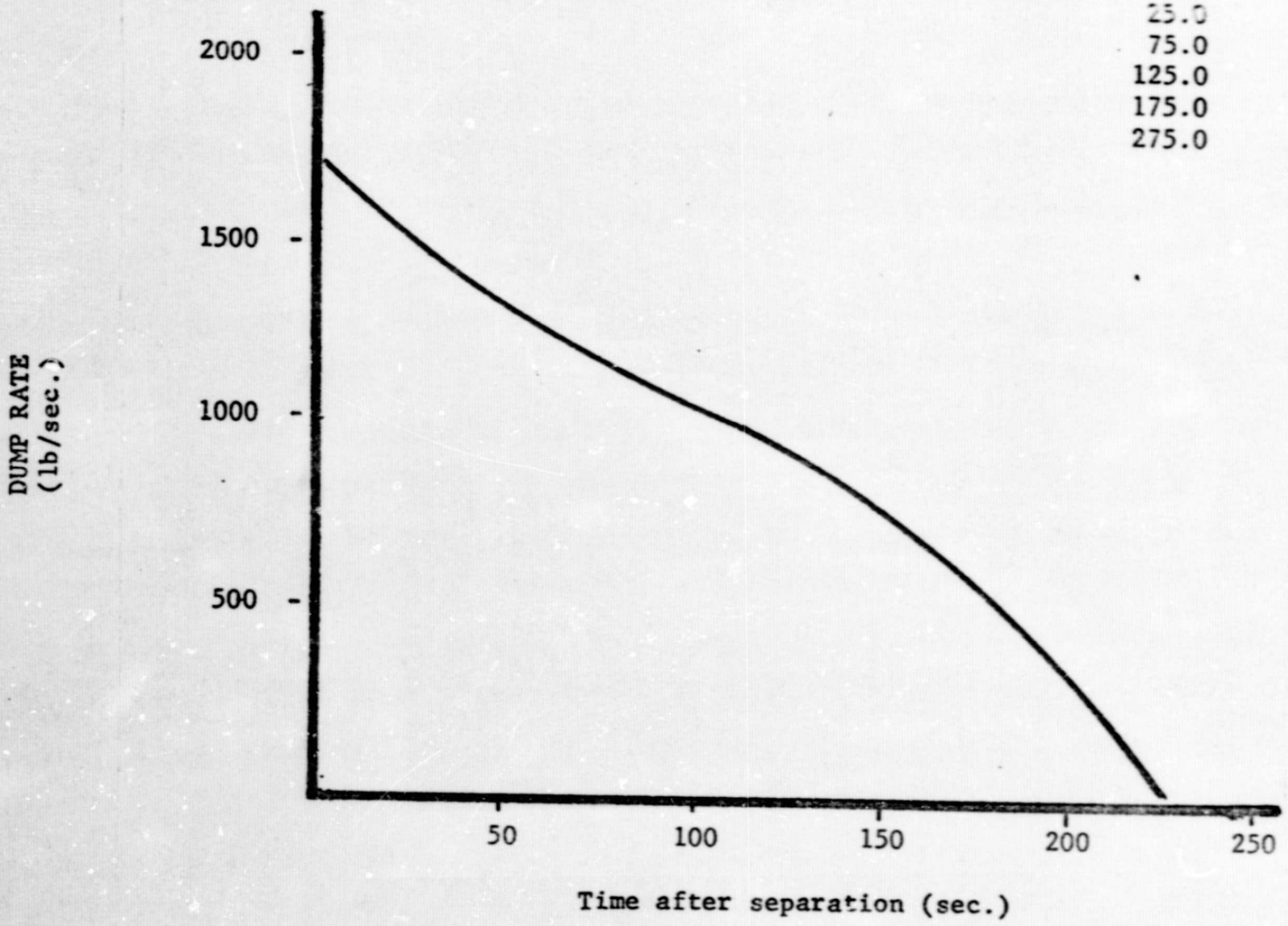

FIGURE C-3

ORBITAL DUMP RATE FOR ONE ENGINE ORBITER CONFIGURATION

TIME OF ABORT AFTER SEPARATION	DUMP TIME	DUMP RATE
0.0	92.4	3077.68
25.0	92.7	2880.56
75.0	87.8	2305.01
125.0	78.4	1758.38
175.0	72.7	1008.86
225.0	107.3	881.98

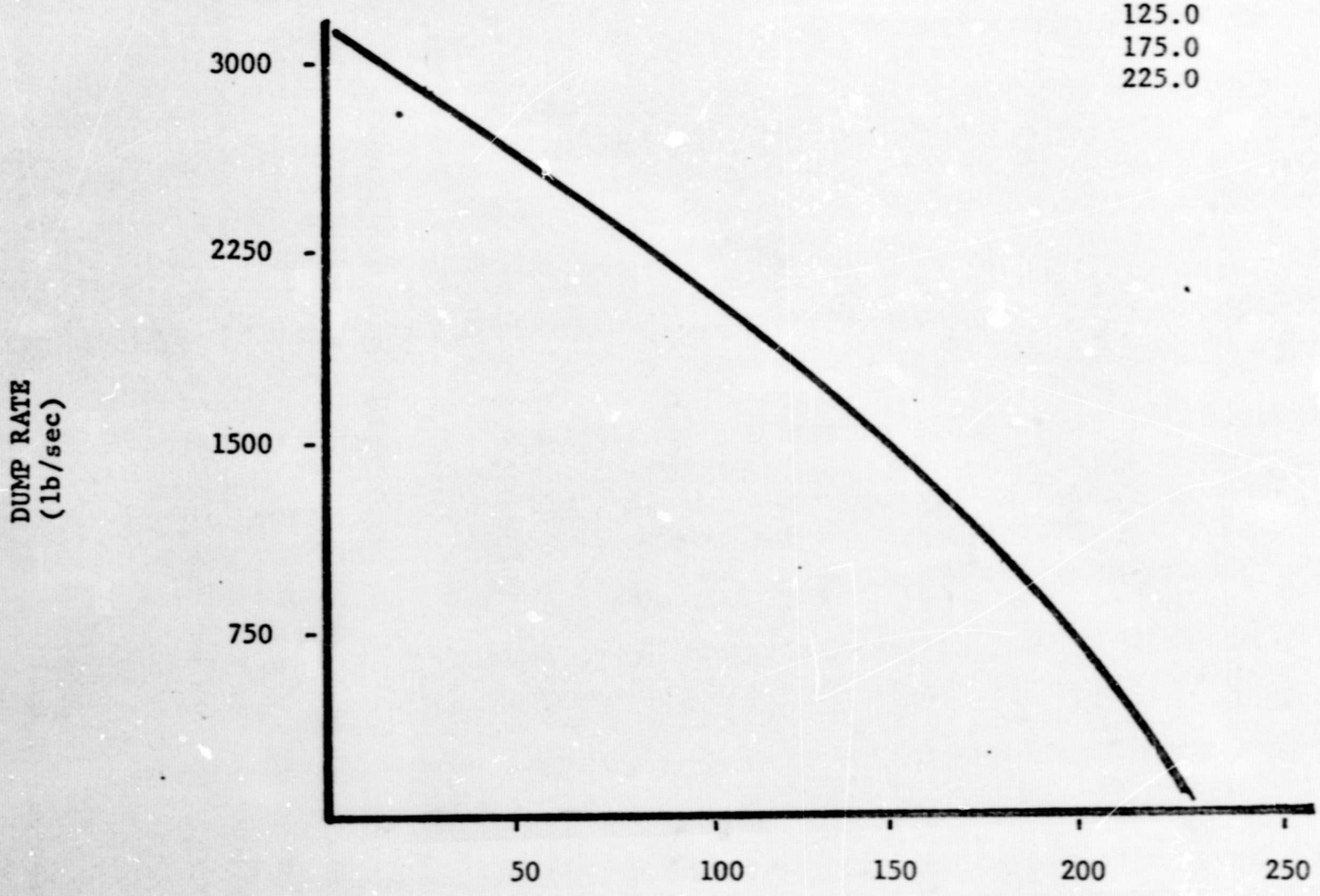

FIGURE C-4

ORBITAL DUMP RATE FOR TWO ENGINE ORBITER CONFIGURATION

A) NORMAL BOOST CONFIGURATIONS

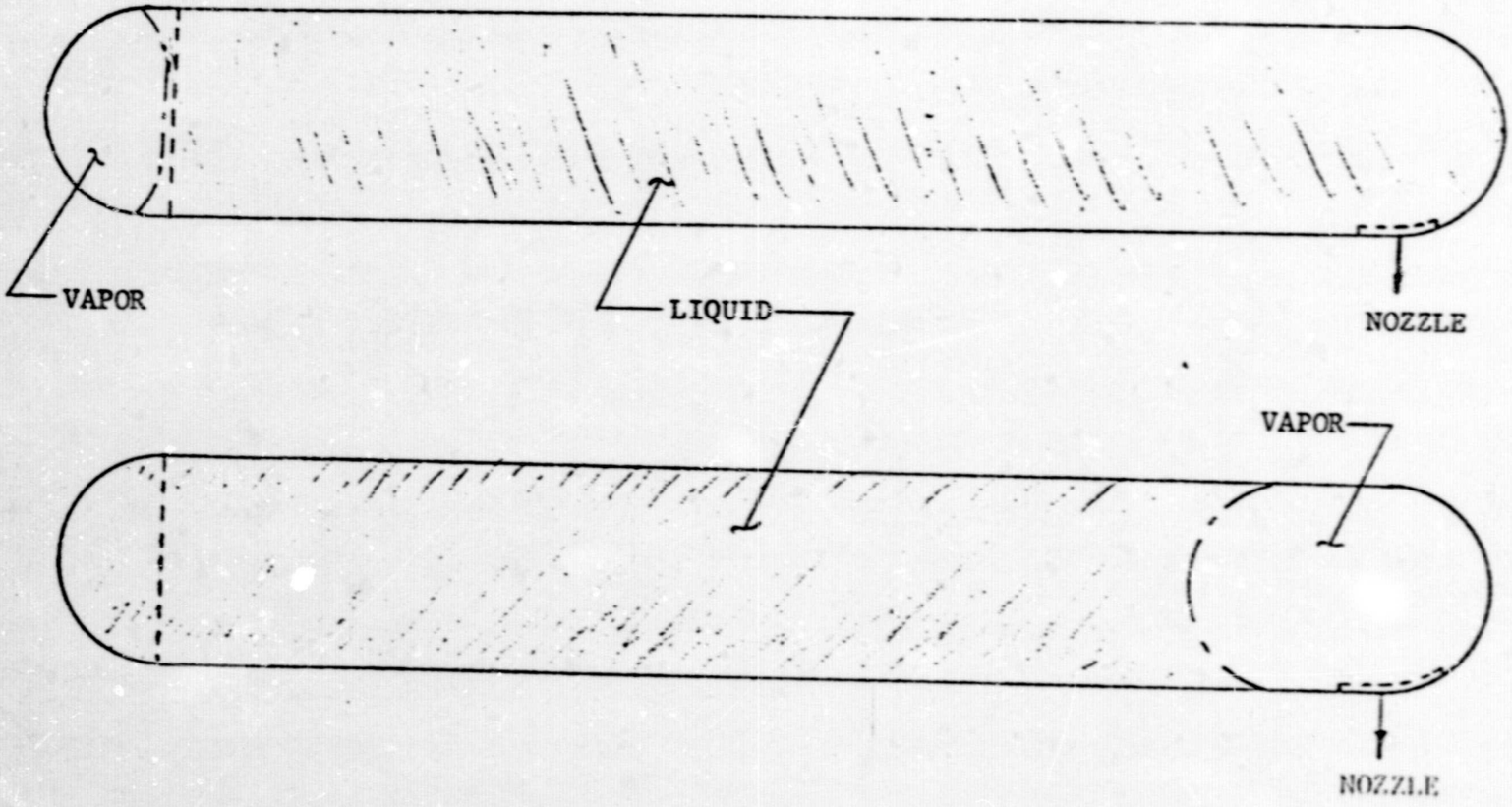

B) CONFIGURATION IN ABORT REGIME AFTER ROCKET BURN

FIGURE C-5

POSSIBLE LIQUID CONFIGURATION IN NORMAL AND ABORT REGIMES

D. Academic

During the summer semester, 1970, the members of the NASA-LSU Space Shuttle Team were required to enroll in ME 208 a graduate course in orbital mechanics. The course, taught by Dr. Mehdy Sabbaghian, was prepared to introduce the student to the problems of orbit maneuvers and rocket performance.

The outline of the semester follows:

1. Introduction to dynamics through vector manipulation
2. Geometric and physical characteristics of orbits
3. Orbital transfer maneuvers
4. Orbital rendezvous
5. Rocket performance
6. Effects of thrust vector misalignment through center of gravity
7. Optimum design of multistage rockets
8. Orbital insertion

As a part of section 4 of the course, each student was required to devise and test a computer program to calculate needed velocity change maneuvers for orbit transfer and rendezvous.

III. REFERENCES

1. Handbook of Mechanical Spring Design, Associated Spring Corp., 1964.

2. Timoshenko, S. and Woinowsky-Krieger, Theory of Plates and Shells, McGraw-Hill Book Company, New York, 1959.

3. Roark, R. J., Formulas for Stress and Strain, McGraw-Hill Book Company, New York, 1965.

4. "Graduate Engineering Practice in Mechanical Engineering--Spring Semester, 1970" by Mechanical, Aerospace & Industrial Engineering Department, Louisiana State University, June 5, 1970.

5. Walburn, A. B. and E. A. Evens, "Residual Propellant Orbital Thermodynamics Program (Reporter) Version A," General Dynamics Report No. GDC-DDB67-004, Convair Division of General Dynamics (1967).

6. "D-C-3 Space Shuttle Study - Volume I" by Engineering and Development Directorate, Manned Spacecraft Center, National Aeronautics and Space Administration, April 27, 1970.

7. DeBrock, S. C., "Development of a Capillary Propellant Management System for a Sixty-Two Inch Spherical Hydrazine Propellant Tank," AIAA Monographs, Vol. 6 Low Gravity Propellant Orientation and Expulsion, 1968.

8. Toole, L. E. and L. J. Hastings, "Behavior of a Sloshing Subjected to a Sudden Reduction in Axial Acceleration," AIAA Monographs, Vol. 6 Low Gravity Propellant Orientation and Expulsion, 1968.

9. DiPeri, L. J., "A Resume of the Management of Liquid Gas Interface Using Surface Tension Technology," AIAA Monographs, Vol. 6 Low Gravity Propellant Orientation and Expulsion, 1968.

10. Bhuta, P. G. and R. L. Johnson, "Zero-G Cryogenic Liquid Expulsion Device," AIAA Monographs, Vol. 6 Low Gravity Propellant Orientation and Expulsion, 1968.

11. Hollister, M. P., "Considerations of Propellant Expulsion With Passive Surface Tension Techniques," AIAA Monographs, Vol. 6 Low Gravity Propellant Orientation and Expulsion, 1968.